Biochemical and Biophysical Research Communications 414 (2011) 14–19

Contents lists available at SciVerse ScienceDirect

Biochemical and Biophysical Research Communications

journal homepage: www.elsevier.com/locate/ybbrc

Exploring the activation mechanism of TRPM8 channel by targeted MD simulations

Alessandro Pedretti [a], Alessandra Labozzetta [a], Matteo Lo Monte [a], Andrea R. Beccari [b], Alessio Moriconi [b], Giulio Vistoli [a,*]

[a] Dipartimento di Scienze Farmaceutiche "Pietro Pratesi", Facoltà di Farmacia, Università degli Studi di Milano, Via Mangiagalli, 25, I-20133 Milano, Italy
[b] Research & Development Centre, Dompé s.p.a., Via Campo di Pile, 67100 L'Aquila, Italy

ARTICLE INFO

Article history:
Received 24 August 2011
Available online 6 September 2011

Keywords:
TRPM8 channel
Menthol
Voltage sensor module
Pore opening
Docking analysis
MD simulations

ABSTRACT

The TRPM8 cation channel belongs to the superfamily of transient receptor potential (TRP) channels. It is involved in non-painful cool sensation and triggered by diverse chemical and physical stimuli whose precise activation mechanism is still unknown. The study presents a set of targeted molecular dynamics (MD) simulations involving selected complexes of the TRPM8 channel whose homology model was recently generated by some of us. More in detail, the MD simulations concerned the TRPM8 alone and in complex with agonists and antagonists. These simulations were focused on voltage sensor module and designed to validate the ligand induced activation mechanism as hypothesized in our previous study. The obtained results are in encouraging agreement with the proposed mechanism and allow a clear discrimination between agonists and antagonists. In addition, the MD runs confirm that the agonist binding triggers a set of concatenate conformational shifts which induce the approaching of the S3 segment toward the S4 segment and culminate in an extension of the latter. By introducing suitable constraints, the reported MD simulations were rendered as fast as possible in order to achieve a truly productive compromise between reliability and computational costs. The obtained results emphasize that suitably targeted MD runs can be fast enough to be systematically applied to predict the bioactivity of large datasets providing it as an useful tool in rational ligand design process.

1. Introduction

The transient receptor potential channel TRPM8 is a nonselective cation channel activated by mild cold (in the range 15–30 °C), voltage, compounds evoking cooling sensations such as menthol and icilin and phosphatidylinositol-4,5-bisphosphate (PIP2), a general activator of ion channels [1,2]. TRPM8 is mostly expressed in somatosensory neurons and acts as a non-painful cooling sensor as demonstrated by knockout mice which exhibit strong deficits in environmental cool sensation. TRPM8 is found also in prostate, bladder and male genital tract thus suggesting additional physiological roles [3,4]. Lastly, TRPM8 expression markedly increases in several tumor cells although the mechanism by which TRPM8 influences the cellular differentiation is still unclear [5].

The TRPM8 gene encodes for a 1104-residue transmembrane protein, whose functional quaternary structure is a homotetramer channel [6]. The transmembrane portion is formed by six helices (termed S1–S6). The first four helices (S1–S4) constitute the voltage sensor module and include the binding sites for menthol and icilin, although they do not fully overlap, since most residues involved in menthol recognition are located in S2, [7] whereas icilin interacts also with residues of S3 [8]. The last two TM helices (S5–S6) constitute the pore module, which is characterized by a highly conserved hydrophobic region and a conserved aspartate residue, whose neutralization results in a non-functional channel. Moreover, the S6 helix is responsible for the ion selectivity of TRPM8 since the introduction of positively charged residues switches from cation to anion selectivity [9,10].

The polymodal mechanism of the TRPM8 activation is still unclear although several studies emphasized the key role of S4 helix and S4–S5 linker which act as a voltage sensor integrating thermal and chemical stimuli. Specifically, mutagenesis studies revealed that the neutralization of the positively charged residues, which characterize these segments, alters voltage dependence and thermal sensitivity and affects menthol binding and activation thus suggesting a general activation mechanism based on conformational shifts happening in this region [10]. This hypothesis is in agreement with the finding that the S4 helix of voltage-dependent phosphatase undergoes a conformational shift during the channel activation from the standard α helix to a more elongated 3_{10} helix suggesting that the activation may involve an elongation of the S4 segment [11]. The proposed role of S4 is also in line with the evidence that opening of the pore does not require conformational changes in S5 or S6 but is based on a rigid-body movement of the entire module [12].

* Corresponding author. Fax: +39 02 19359.
E-mail address: Giulio.Vistoli@unimi.it (G. Vistoli).

0006-291X/$ - see front matter © 2011 Elsevier Inc. All rights reserved.
doi:10.1016/j.bbrc.2011.08.134

Starting from these evidences, a full-length homology model in its homotetrameric form was recently generated and the possible effects of ligand binding on the conformation of the S4 helix and S4–S5 linker were then investigated [13]. This study allowed hypothesizing that ligand binding breaks a key H-bond in the TRPM8 binding cavity and this change induces an approach of the S3 helix towards S4 helix and promotes the S4 elongation to a 3_{10} helix conformation. This conformational shift, which can be induced also by the voltage effect on positively charged residues in S4, impacts on the arrangement of the S4–S5 linker and induces a movement of the S5–S6 pore module with resulting channel opening. The proposed mechanism can also account for the modularity of channel opening which may depend on how many residues of the S4 segment shift to 3_{10} helix [14].

With a view to substantiating the hypothesized mechanism, this study involved a set of molecular dynamics (MD) simulations of the TRPM8 monomer alone and in complex with selected ligands. To avoid too long simulations, the MD runs were intentionally targeted so as to focus the attention on the conformational shifts directly induced by ligand binding (namely, the approaching of S3 towards S4 and the shifts of the latter). Thus, the performed simulations should clarify the role of the early conformational changes which trigger (or prevent) channel opening and, at the same time, they should be fast enough to be systematically used to investigate the bioactivity of large ligand datasets.

2. Materials and methods

2.1. Complexes set-up

The simulations are based on the TRPM8 homology model as recently generated by some of us [13]. Briefly, the model for the TRPM8 monomer was built by fragments [15] using the experimental structure of the Kv1.2 Shaker channel [16] as the global template for the TM region, while the C-terminal domain was constructed using the experimental structure of HCN2 pacemaker channel as the template [17]. Next, the tetramer was modeled by automatic protein–protein docking simulations and the optimized structure was used in docking analyses.

The present study involved four MD simulations considering the TRPM8 alone and in complex with menthol, icilin and AMTB, a known TRPM8 antagonist. While the choice of the representative agonists (namely, menthol and icilin) was quite obvious involving the most known natural and synthetic compounds, AMTB was chosen considering that a recent mutational analysis suggested that some hydrophobic inhibitors (such as capsazepine and BCTC) interact in a lateral binding cavity which only marginally overlaps with the orthosteric binding site [18], whereas the more polar AMTB should occupy the orthosteric cavity in a competitive manner [19].

The complexes with menthol and icilin were taken from the previous study [13] while the one with AMTB was derived by docking simulations. Specifically, AMTB was considered in its protonated form and the conformational profile investigated by a clustered MonteCarlo analysis as implemented in VEGA suite of programs [20] to produce 1000 minimized conformers. The lowest energy structure was exploited in docking analysis by AutoDock 4.0 considering a sphere of 12.0 Å radius around Tyr745 so encompassing the entire binding cavity. The resolution of the grid was $40 \times 50 \times 60$ points with a grid spacing of 0.610 Å. The ligand was docked into this grid with the Lamarckian algorithm as implemented in AutoDock and the flexible bonds of the ligand were left free to rotate. The genetic-based algorithm ran 20 simulations per substrate with 2000,000 energy evaluations and a maximum number of generations of 27,000. The crossover rate was increased to 0.8, and the number of individuals in each population to 150. All other parameters were left at the AutoDock default settings [21].

2.2. MD simulations

The MD simulations lasted 5 ns and involved TRPM8 alone and bound to menthol, icilin and AMTB. To simplify the simulation space, the MD runs involved a single monomer and all atoms were kept fixed apart from those within a sphere of 15 Å radius around the bound ligand. This sphere was chosen to include the lower region of the transmembrane voltage sensor (S1–S4) plus the S4–S5 linker. The simulations had the following characteristics: (a) Newton's equation was integrated using the r-RESPA method (every 4 fs for long-range electrostatic forces, 2 fs for short-range non bonded forces, and 1 fs for bonded forces); (b) the presence of the membrane bilayer was implicitly accounted for by setting the dielectric constant to 10.3 (namely, the experimental value for *n*-octanol) (c) the pressure exerted by the adjacent monomers was indirectly simulated by introducing the Periodic Boundary Conditions (65 Å × 75 Å × 80 Å); (d) the long-range electrostatic potential was treated by the Particle Mesh Ewald summation method ($65 \times 75 \times 80$ grid points); (e) the temperature was maintained at 300 ± 10 K by means of the Langevin's algorithm; (f) Lennard–Jones (L–J) interactions were calculated with a cut-off of 10 Å and the pair list was updated every 20 iterations; (g) a frame was stored every 5 ps, to yield 1000 frames. The simulations were carried out in two phases: an initial period of heating from 0 to 300 K over 300,000 iterations (300 ps, i.e. 1 K/ps) and the monitored phase of 5 ns. All MD runs were carried out using Namd2.7 [22] with the force-field CHARMm v22 and Gasteiger's atomic charges on a 16-core Tyan VX-50 system.

3. Results

As a preamble, it should be reminded that in the previous paper the following three-step activation mechanism was hypothesized [13]. First, the agonist strongly interacts with Tyr745 disrupting its initial interaction with Asp802. Second, the free Asp802 residue approaches Arg842 and, third, this last shift results in an extension of the S4 segment which, in turn, induces the opening movement of the pore module. Accordingly, the analysis of the performed simulations was focused on: (a) the moving away between Tyr745 and Asp802; (b) the approaching of Asp802 to Arg842; and (c) the resulting conformational changes in the S4 segment.

Fig. 1 reports the dynamic profiles for the distance between Tyr745 and Asp802 showing that the starting conformation of all simulated complexes is similarly stabilized by a close contact between Tyr745 and Asp802. Nevertheless, the four simulations show quite different behaviors. Indeed, while the free TRPM8 and the channel bound to AMTB conserve the contact during the whole simulation, the binding with menthol and icilin disrupts this interaction and the monitored distance progressively increases during the simulation. Moreover, Fig. 1 shows that menthol induces a slower but more pronounced conformational shift compared to that exerted by icilin.

The monitored differences could be somewhat explained by a visual comparison of the first and last frames of the monitored simulations. During the simulation time, both agonists reinforce their interaction with Tyr745 through the hydroxyl function for menthol and through the nitro group and the pyrimidinone ring for icilin. Due to its small size and hydrophobic nature, menthol appears to be wedged in the binding site physically distancing Tyr745 from Asp802 and explaining the significant increases as seen in Fig. 1. Despite its polarity, AMTB, conversely, engages the TRPM8 binding site mainly stabilizing π–π stacking and charge transfer interactions

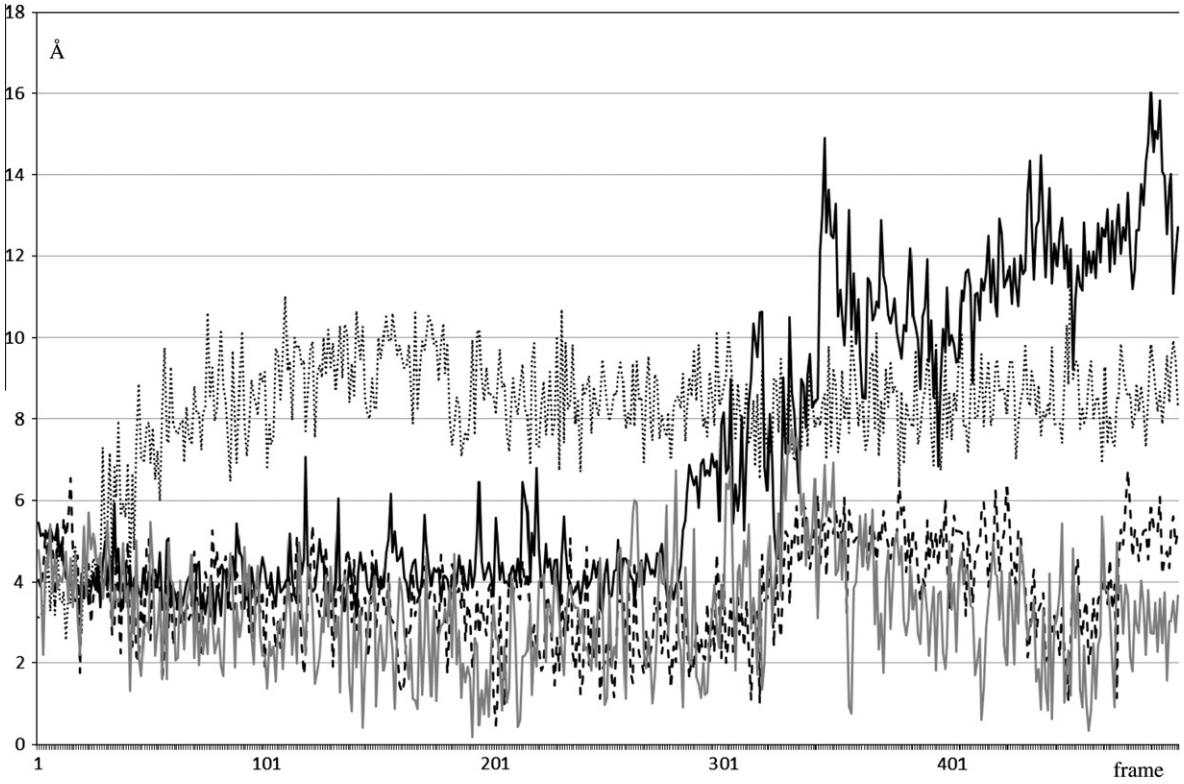

Fig. 1. Dynamic profile for the distance between Tyr745 and Asp802 as monitored in the four MD simulations (color legend: gray line = TRPM8 alone, black line = TRPM8 in complex with menthol, dotted line = TRPM8 in complex with icilin; dashed line = TRPM8 in complex with AMTB antagonist).

and it never contacts Tyr745 or Asp802 during all the monitored simulation.

Taken together, these results seem to confirm that TRPM8 agonists are characterized by ability to strongly engage Tyr745, thus liberating Asp802 which in turn can approach Arg842, while the antagonists, irrespective of their polarity, occupy the binding site or block the entrance, as recently proposed by Malkia [18], without contacting Tyr745 nor influencing its interaction with Asp802. This result shows that the performed simulations can clearly discriminate between agonists and antagonists and affords an interesting confirmation for the first triggering step of the proposed mechanism.

Concerning the approaching of Asp802 towards Arg842, Fig. 2 reports the distance between these residues as monitored during the MD runs. One may note that all complexes are characterized by an initial distance of about 10–12 Å which indicates a lack of significant interactions between them. As already seen in Fig. 1, also Fig. 2 shows marked differences between the performed simulations. Indeed, while the distance between Asp802 and Arg842 remains constantly above 10 Å during the entire simulations of the TRPM8 free and bound to the AMTB antagonist, the simulated agonists induce a clear approaching characterized by a distance between Asp802 and Arg842 of about 5 Å thus indicating a relevant ionic interaction between them. Remarkably, the timing of the approaching of Asp802 towards Arg842 as seen for the agonist complexes is in line with that of moving away between Tyr745 and Asp802 as reported by Fig. 1. This observation seems to confirm that the two monitored structural changes can be seen as related steps of a concerted mechanism activated by agonists and leading to the channel opening.

The last analysis involved the conformational shifts which happen in the S4 segment due to the agonist binding. To simplify the analysis and considering that the imposed constraints could alter the exact movements of this segment, the attention was simply focused on the atomic fluctuations as described by RMSD values computed taking into account only the S4 atoms and irrespective of the conformational shifts underlying such fluctuations. Fig. 3 depicts the dynamic profile of the RMSD values showing interesting differences between the monitored simulations. Indeed, after a common starting equilibration phase, the S4 segment evidences a clearly greater mobility when the channel is bound to agonists compared to TRPM8 alone or bound to AMTB. Yet again, there is an evident synchronization between the RMSD variations induced by the simulated agonists and the conformational shifts as analyzed by Figs. 1 and 2. Indeed, the RMSD increase occurs almost immediately with icilin and after about 3 ns with menthol. This further confirms that the monitored structural variations can be seen as sequential steps of the same activation mechanism selectively induced by the agonist binding. A visual inspection of the dynamic profile for the S4 segments does not allows clear conformational shifts to be detected, probably because they are hampered by the imposed constraints resulting in chaotic atomic fluctuations. Nevertheless, it should be observed that such disordered movements can be seen only when the channel is bound to an agonist thus suggesting that they should be indicative of the S4 conformational shifts occurring during the TRPM8 activation mechanism.

To summarize what previously discussed, Fig. 4 compares the last frame of MD run of TRPM8 in complex with AMTB (Fig. 4A) with that of TRPM8 with icilin (Fig. 4B). The former is quite similar to the last frame of MD run for the free channel (results not shown) which, in turn, is comparable with the starting structure of all the considered simulations. Indeed, the key residues involved in channel activation do not evidence significant shifts during the simulations without agonists. In detail, Fig. 4A shows that the AMTB complex is stabilized by a key charge transfer interaction with

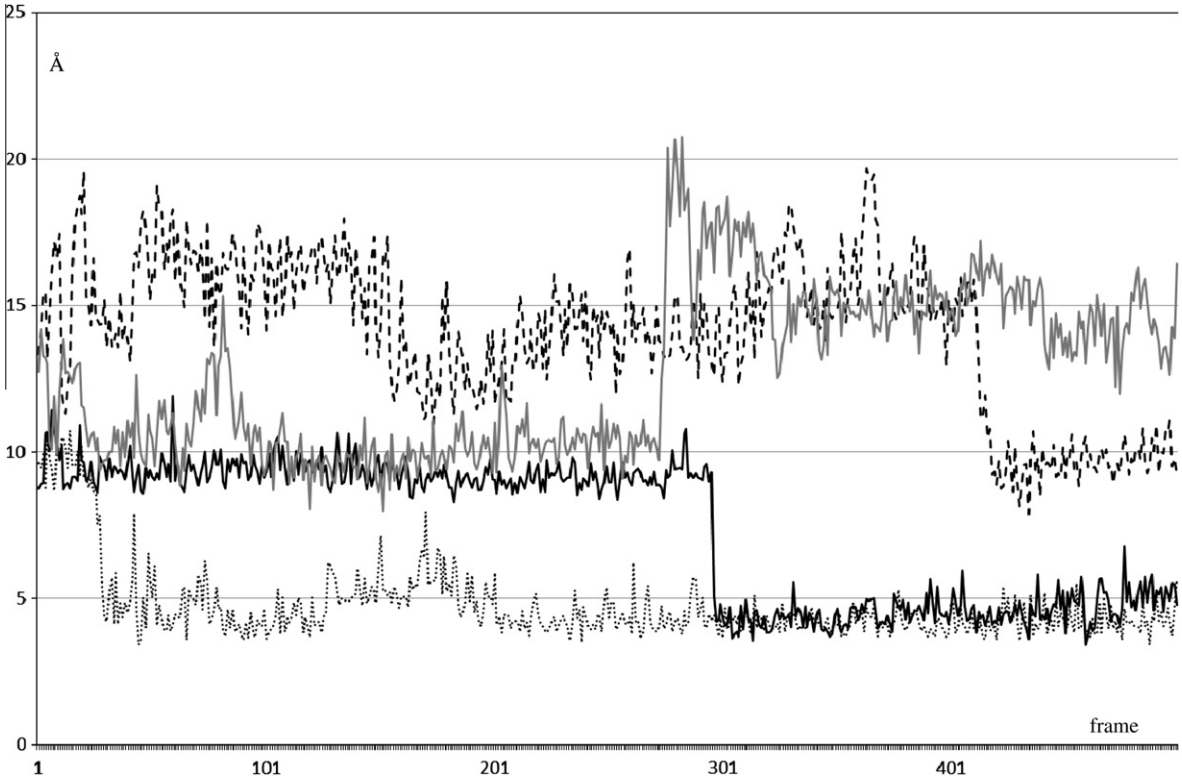

Fig. 2. Dynamic profile for the distance between Asp802 and Arg842 as monitored in the four MD simulations (The color legend is the same as in Fig. 1).

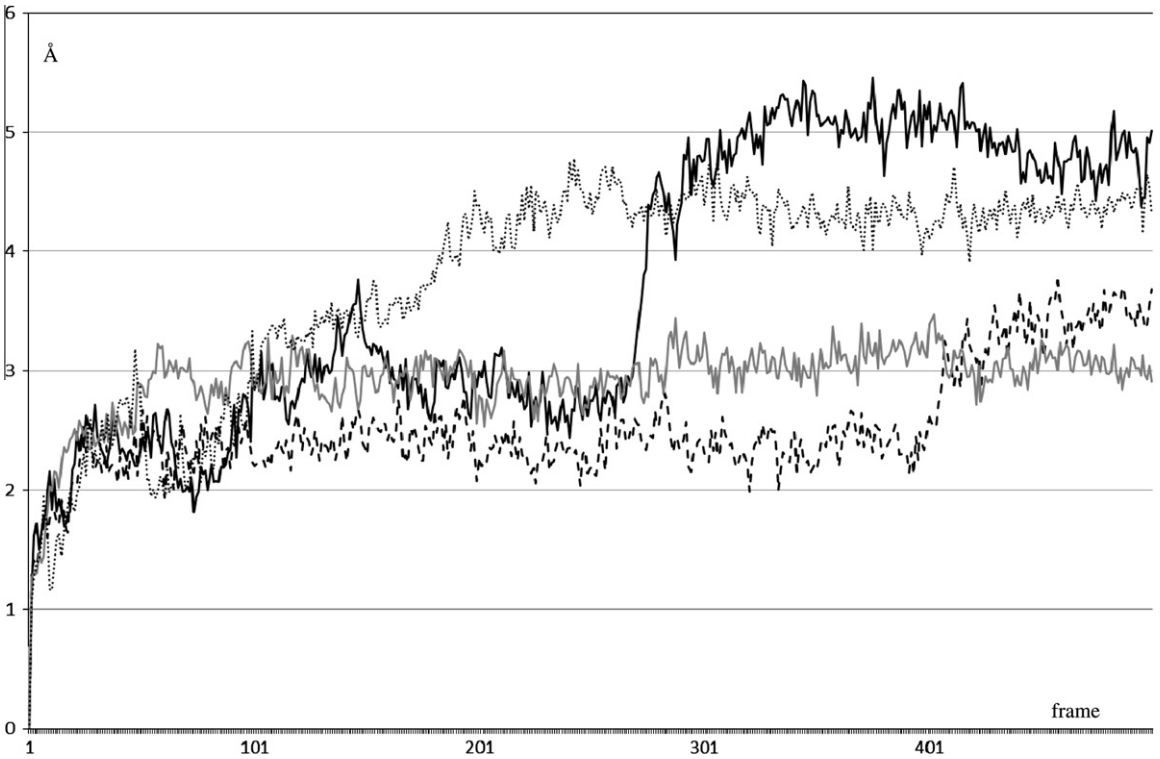

Fig. 3. Dynamic profile for the RMSD values as computed for the S4 atoms only in the four MD simulations (The color legend is the same as in Fig. 1).

Arg816 plus a set of hydrophobic and π/π contact with apolar residues surrounding the binding site (not depicted for clarity apart from Trp740) but it does not contact Tyr745, which indeed remains reasonably close to Asp802. Consequently, Asp802 cannot approach Arg842, whose resting arrangement appears to be stabilized by a H-bond with Thr803. Conversely, Fig. 4B shows that icilin strongly attracts Tyr745 mostly through a H-bond with the ligand's nitro group and such an interaction makes Asp802 free to approach

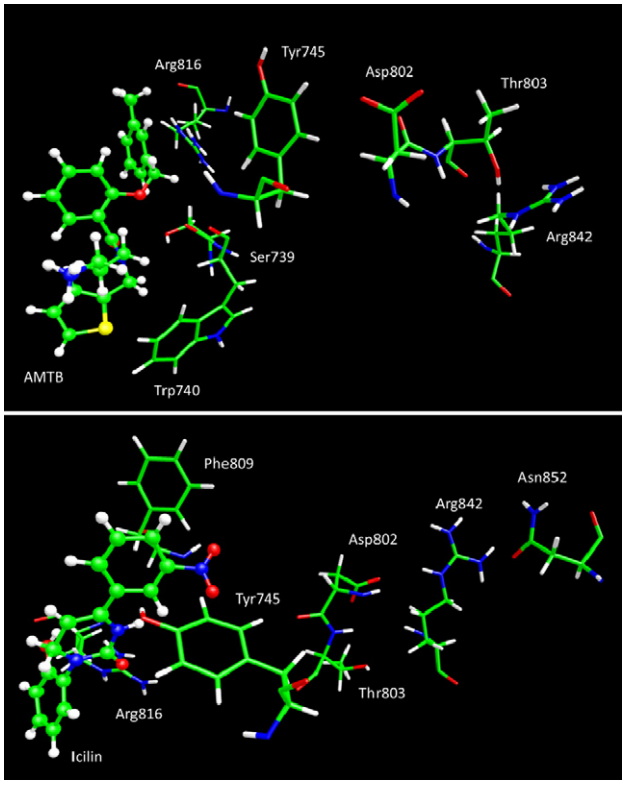

Fig. 4. Comparison of the arrangement of the key residues involved in the proposed activation mechanism between the last frame of TRPM8 in complex with AMTB (Fig. 4A) and with icilin (Fig. 4B). In the latter, the crucial approaching of Asp802 towards Arg842 can be observed.

Arg842. Notably, the final pose of Arg842 is also stabilized by a H-bond with Asn852. Considering that Asn852 is markedly distant from Arg842 in the last frame of MD run with AMTB (~10.5 Å), such an approach could exemplify the reported atomic fluctuations observed in the S4 segment only when the channel is bound to an agonist.

With the aim to obtain an overall picture of the conformational changes which characterize the entire TRM8 monomer, Table 1 compares the relative abundance of secondary motifs of the first frame of MD run involving the TRPM8 alone (taken as representative of all starting structures) with that of the last frame of the performed simulations. One may note that the main difference involves the relative abundance of helical motifs. Indeed, while the abundances of strand and turn motifs are rather constant in the examined frames, the helical motifs decrease specifically during the MD runs of TRPM8 in complex with agonists with a resulting increase of the coil abundance. These variations may reflect the atomic fluctuations induced by agonist activation and which mostly involve the S4 segment.

Table 1
Comparison of the relative abundance of main secondary motifs (expressed as percentage values and computed by Stride only for the unconstrained atoms) for the starting and last frames of the monitored MD simulations.

Motif	Starting free	Final free	Final menthol	Final icilin	Final AMTB
Helices	39.5	35.4	31.6	31.3	36.4
Strand	1.4	0.00	1.4	1.7	1.4
Turn	15.8	17.2	14.4	13.7	16.5
Coil	43.3	47.4	52.6	53.3	45.4

4. Discussion

The study concerns a set of targeted MD simulations of TRPM8 alone as well as in complex with both agonists and antagonists with a view to validating the recently hypothesized mechanism of activation [13]. The obtained results afford encouraging confirmations for this mechanism revealing significant differences between the performed MD runs. Indeed, these simulations clearly discriminate between agonists and antagonists since only the formers are able to induce a set of conformational shifts which culminate in an increased S4 mobility and should trigger the channel opening. More in detail, the performed simulations proved successful in reproducing the early conformational shifts which induce the channel activation, whereas a suitable analysis of the S4 mobility would require less constrained and more comprehensive MD simulations. Nevertheless and to the best of our knowledge, this is the first computational study investigating the ligand-induced activation mechanism involving the voltage sensor module of the TRP channels also because the previous computational studies on similar cationic channels had been mainly focused on the pore opening as well as on the dynamic behavior of the binding site located within the C-terminal domain [23].

Furthermore, it should be emphasized that these MD runs were purposely targeted to represent an optimal compromise between computational cost and simulation reliability in order to be systematically used to investigate the intrinsic activity of large ligand datasets. Considering that the described simulations are able to conveniently discriminate between agonists and antagonists and require, on average, less than 12 h on a multicore system, they appear particularly suited for a systematic use. Finally, the reported simulations underline that purposely targeted MD simulations can be fertile tools for the rational design of valuable TRPM8 ligands and this appears particularly useful when considering the extremely nonspecific nature of the binding site located on the surface of the voltage sensor module that renders the docking results not easily interpretable.

References

[1] Y. Liu, N. Qin, TRPM8 in health and disease: cold sensing and beyond, Adv. Exp. Med. Biol. 704 (2011) 185–208.
[2] J. Defalco, M.A. Duncton, D. Emerling, TRPM8 Biology and Medicinal Chemistry, Curr. Top Med. Chem. 11 (2011) 2237–2252.
[3] C. Van Haute, D. De Ridder, B. Nilius, TRP channels in human prostate, Sci. World J. 10 (2010) 1597–1611.
[4] K.E. Andersson, C. Gratzke, P. Hedlund, The role of the transient receptor potential (TRP) superfamily of cation-selective channels in the management of the overactive bladder, BJU Int. 106 (2010) 1114–1127.
[5] V. Lehen'kyi, N. Prevarskaya, Oncogenic TRP channels, Adv. Exp. Med. Biol. 704 (2011) 929–945.
[6] M. Li, Y. Yu, J. Yang, Structural biology of TRP channels, Adv. Exp. Med. Biol. 704 (2011) 1–23.
[7] M. Bandell, A.E. Dubin, M.J. Petrus, A. Orth, J. Mathur, S.W. Hwang, Patapoutian, High-throughput random mutagenesis screen reveals TRPM8 residues specifically required for activation by menthol A, Nat. Neurosci. 9 (2006) 493–500.
[8] H.H. Chuang, W.M. Neuhausser, D. Julius, The super-cooling agent icilin reveals a mechanism of coincidence detection by a temperature-sensitive TRP channel, Neuron 43 (2004) 859–869.
[9] F.J. Kühn, G. Knop, A. Lückhoff, The transmembrane segment S6 determines cation versus anion selectivity of TRPM2 and TRPM8, J. Biol. Chem. 282 (2007) 27598–27609.
[10] T. Voets, G. Owsianik, A. Janssens, K. Talavera, B. Nilius, TRPM8 voltage sensor mutants reveal a mechanism for integrating thermal and chemical stimuli, Nat. Chem. Biol. 3 (2007) 174–182.
[11] C.A. Villalba-Galea, W. Sandtner, D.M. Starace, F. Bezanilla, S4-based voltage sensors have three major conformations, Proc. Natl. Acad. Sci. USA 105 (2008) 17600–17607.
[12] N. Bocquet, H. Nury, M. Baaden, C. Le Poupon, J.P. Changeux, M. Delarue, P.J. Corringer, X-ray structure of a pentameric ligand-gated ion channel in an apparently open conformation, Nature 457 (2009) 111–114.
[13] A. Pedretti, C. Marconi, I. Bettinelli, G. Vistoli, Comparative modeling of the quaternary structure for the human TRPM8 channel and analysis of its binding features, Biochim. Biophys. Acta. 1788 (2009) 973–982.

[14] J.A. Matta, G.P. Ahern, Voltage is a partial activator of rat thermosensitive TRP channels, J. Physiol. 585 (2007) 469–482.
[15] A. Pedretti, M. Villa, M. Pallavicini, E. Valoti, G. Vistoli, Construction of human ghrelin receptor (hGHS-R1a) model using a fragmental prediction approach and validation through docking analysis, J. Med. Chem. 49 (2006) 3077–3085.
[16] S.B. Long, E.B. Campbell, R. Mackinnon, Crystal structure of a mammalian voltage-dependent Shaker family K+ channel, Science 309 (2005) 897–903.
[17] W.N. Zagotta, N.B. Olivier, K.D. Black, E.C. Young, R. Olson, J.E. Gouaux, Structural basis for modulation and agonist specificity of HCN pacemaker channels, Nature 425 (2003) 200–205.
[18] A. Malkia, M. Pertusa, G. Fernández-Ballester, A. Ferrer-Montiel, F. Viana, Differential role of the menthol-binding residue Y745 in the antagonism of thermally gated TRPM8 channels, Mol. Pain. 5 (2009) 62.
[19] E.S. Lashinger, M.S. Steiginga, J.P. Hieble, L.A. Leon, S.D. Gardner, R. Nagilla, E.A. Davenport, B.E. Hoffman, N.J. Laping, X. Su, AMTB a TRPM8 channel blocker: evidence in rats for activity in overactive bladder and painful bladder syndrome, Am. J. Physiol. Renal. Physiol. 295 (2008) 803–810.
[20] A. Pedretti, L. Villa, G. Vistoli, VEGA: a versatile program to convert handle and visualize molecular structure on Windows-based PCs, J. Mol. Graph. 21 (2002) 47–49.
[21] G.M. Morris, D.S. Goodsell, R.S. Halliday, R. Huey, W.E. Hart, R.K. Belew, A.J. Olson, Automated docking using a lamarckian genetic algorithm and and empirical binding free energy function, J. Comput Chem. 19 (1998) 1639–1662.
[22] L. Kalé, R. Skeel, M. Bhandarkar, R. Brunner, A. Gursoy, N. Krawetz, J. Phillips, A. Shinozaki, K. Varadarajan, K. Schulten, NAMD2: greater scalability for parallel molecular dynamics, J. Comp. Phys. 151 (1999) 283–312.
[23] L.G. Cuello, V. Jogini, D.M. Cortes, A.C. Pan, D.G. Gagnon, O. Dalmas, J.F. Cordero-Morales, S. Chakrapani, B. Roux, E. Perozo, Structural basis for the coupling between activation and inactivation gates in K(+) channels, Nature 466 (2010) 272–275.